Chapter 8
The Mathematics of Chaînes Opératoires

P. Jeffrey Brantingham

Abstract The decision-making processes underlying core reduction are often framed in terms of the execution of different complex, integrated technological designs. This chapter adopts an alternative approach of specifying simple, independent technological decisions deployed during reduction. These are used to develop three mathematical models of core reduction of increasing complexity. The modeled technologies are labeled as Bernoulli, Markov, and Price cores after their fundamental mathematical properties. Expectations concerning core reduction intensity are derived and tested using data from Paleolithic sites in Africa and Asia.

Introduction

Many inferences about Paleolithic behavior, culture, adaptation, and hominin cognitive capacities hinge on the analysis of stone technological design. In general, the number of technological actions involved in core reduction, the orders in which they are deployed, and the ways in which they are combined are taken as proxy measures of such things as time, energy, or risk optimization in foraging (Beck et al. 2002; Kuhn 1994; Nelson 1991), cultural transmission (Kuhn 2004; Lycett 2008), and planning depth or spatial cognitive modules (Delagnes and Roche 2005). However, any sizable archaeological assemblage usually contains cores and debitage representing tremendous variability in the intensity of reduction; some cores are intensively reduced and discarded in "spent" condition, while other cores discarded seemingly with abundant remaining use life. Idealized technological designs are therefore implemented with tremendous variability and, it is fair to say, many behavioral, adaptive, and cognitive models of hominin behavior have not taken the variability in core reduction sufficiently into account. Here, I seek a formalization of the processes leading to variability in core reduction intensity and, ultimately, core design.

P.J. Brantingham (✉)
Department of Anthropology, UCLA, 341 Haines Hall, Los Angeles, CA 90095, USA
e-mail: branting@ucla.edu

S.J. Lycett and P.R. Chauhan (eds.), *New Perspectives on Old Stones: Analytical Approaches to Paleolithic Technologies*, DOI 10.1007/978-1-4419-6861-6_8,

Bernoulli Core Technology

At an elementary level, the process of stone core reduction consists of directing force at a mass of stone to remove a sharp-edged "flake" (detached piece) that may then be used in one or more activities. The detached piece of stone is presumed to have economic utility, which may be measured in a number of interdependent currencies including product shape (Boëda 1995; Elston and Brantingham 2003), weight (Beck et al. 2002; Kuhn 1994), edge length (Brantingham and Kuhn 2001), or resharpening potential (Bamforth 2002; Dibble 1995). As a simple starting point, core reduction may be modeled as a series of Bernoulli trials, where each detached piece removed from the core either meets a predetermined utility criterion (i.e., a success) or it does not (i.e., a failure). This model requires that the probability of producing a detached piece meeting the utility criterion is fixed, usually endogenously, and that each removal is independent of both the preceding and any subsequent removals. Under these conditions, the process of core reduction is completely specified by the negative binomial distribution.

$$P(N = X) = \binom{N-1}{n-1} p^n (1-p)^{N-n}, \tag{8.1}$$

where N is the number of flake removals necessary to produce n detached pieces meeting the utility criterion and p is the independent probability of producing an acceptable product with each attempted removal. For example, given a probability of success in any given flake removal attempt $p = 0.6$, then Eq. 8.1 indicates that the probability of producing 18 acceptable products in 20 total removals is $P(N = 20) = 0.09$. The probability of a success p in this context may be interpreted as a measure of raw material quality.

Mean core reduction intensity is given by $\mu = n/p$, while the variance is given by $\sigma^2 = n(1-p)/p^2$. Surprisingly, neither of these quantities are dependent upon the maximum number of flakes that can be removed from a core, though maximum use life is an implicit benchmark in many economic analyses of core reduction and is assumed to be an influence on reduction intensity (Brantingham and Kuhn 2001; Braun et al. 2008; Dibble and Bar-Yosef 1995). In the Bernoulli core model, the mean and variance in expected reduction intensity are dependent *only* upon the endogenous probability of a success p and the number of successful products n sought, which may be much less (or much more) than the maximum possible products N that could be produced by a core.

The Bernoulli core model predicts that mean core reduction intensity increases as the probability of a success decreases. Consider a hypothetical assemblage of cores, based on different raw material types, all of which are directed at producing a minimum of ten successful products (Fig. 8.1a). Cores based on the high-quality raw material, which has an endogenous probability of producing a successful flake $p = 0.7$, are expected to have a mean reduction intensity of 14.29 removals. In contrast, cores based on the intermediate quality raw material ($p = 0.5$) are expected

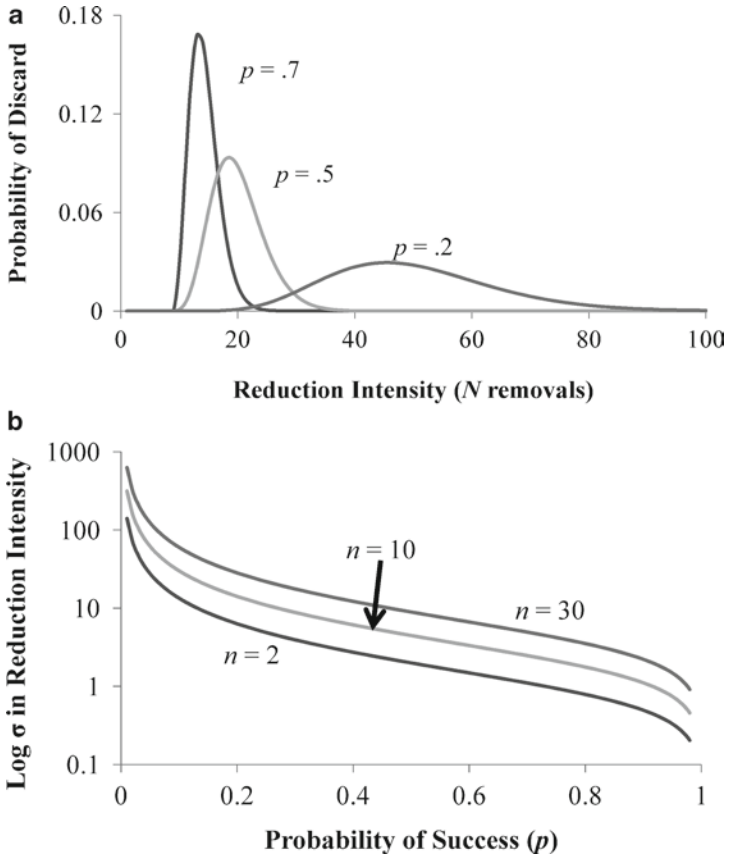

Fig. 8.1 (**a**) Raw materials characterized by high probabilities of success (i.e., low probability of reduction errors) will display low mean reduction intensity. Illustrated are the probability distributions for the total number of flakes removed *N* from a core at the point when ten successful flakes *n* are produced (and the core is discarded). Note that the expected mean reduction intensity *n*/*p* coincides with the mode only when the distribution is normal. (**b**) The standard deviation (σ) in core reduction intensity decreases geometrically as the probability of successful flake production increases. Illustrated are three curves for different values of *n*, the number of desired successes

to have a mean reduction intensity of 20 removals. The expected mean reduction intensity for cores based on the lowest quality material ($p = 0.2$) is 50 removals.

The Bernoulli core model also predicts that the standard deviation (σ) in core reduction intensity should decrease rapidly as the probability of success increases (Fig. 8.1b). For example, to obtain ten ($n = 10$) successful products, the standard deviation in core reduction intensity of a Bernoulli core is 30 removals ($\sigma^2 = 900$ removals^2) for a stone raw materials with a low endogenous probability of success $p = 0.1$. A standard deviation of only 1.77 removals ($\sigma^2 = 3.125$ removals^2) is expected for a raw material with a high endogenous probability of success $p = 0.8$.

Evaluating the Bernoulli Core Model

The Bernoulli core model is perhaps best suited to describing reduction intensity in relatively simple core technologies such as Oldowan (Mode I) core-and-flake industries. In particular, one might assume with Oldowan technologies that the probability of producing a successful flake is determined almost entirely by raw material quality (Potts 1991; Stout et al. 2005; Toth 1982). It also may be reasonable to assume that the successful production of an acceptable end product is largely independent of the results of earlier removals, and does not significantly influence the success of subsequent removals (but see Delagnes and Roche 2005). Oldowan (Mode I) core technologies thus may meet the two key assumptions necessary to model core reduction as a series of independent Bernoulli trials.

Figure 8.2 presents boxplots of weight-standardized core flake scar counts, by raw material class, for nine sites located in Olduvai Gorge Bed I and lower Bed II (Kimura 2002). The sites range in age from approximately 1.8 (DK) to 1.2 mya (TK) and include both classic Oldowan and early Acheulean industries. The raw material classes presented are aggregates of several distinct types. Quartz and quartzite materials are combined and generally are considered to be low quality (i.e., low p) because of a tendency for the material to fracture along internal cleavage planes. Fine-grained igneous materials include vesicular lava, phonolite, and basaltic lava. These materials can vary widely in quality depending upon the size and distribution of vesicles and phenocrysts in the rock matrix. When they are relatively fine-grained they are considered to be of intermediate quality (i.e., intermediate p). Finally, fine-grained siliceous rocks such as chert have the highest quality (i.e., highest p) relative to the other materials found in the Oldowan assemblages under consideration. Other stone raw materials present in the Oldowan assemblages such as gneiss are too rare to warrant statistical comparison.

If the assumptions concerning raw material quality are approximately correct, then the Bernoulli core model predicts that the mean and variance in reduction intensity should be lowest for the highest quality materials and, conversely, highest for the lowest quality materials. The data from Olduvai Bed I and II provide at best marginal support for the Bernoulli core model. Considering quartz/quartzite and lava raw materials, core reduction intensity patterns may be as anticipated; lower quality quartz/quartzite cores display both a greater median and greater range of flake scars per gram of raw material compared with the (somewhat) higher-quality lavas (Fig. 8.2). Patterns of core reduction intensity for chert cores, however, fail to conform to predictions. In all but one case (MNK Chert Factory Site), chert cores display both the greatest median and greatest range in reduction intensity of the materials present at the sites.

The reasons for the mixed performance of the Bernoulli core model are twofold. First, the model assumes that a core will be immediately discarded once the target number of acceptable flakes is reached. Second, if the target number of flakes has not been reached, then it is assumed that core reduction will continue even though the core might have little hope of ever producing them. Referring back to Fig. 8.1a,

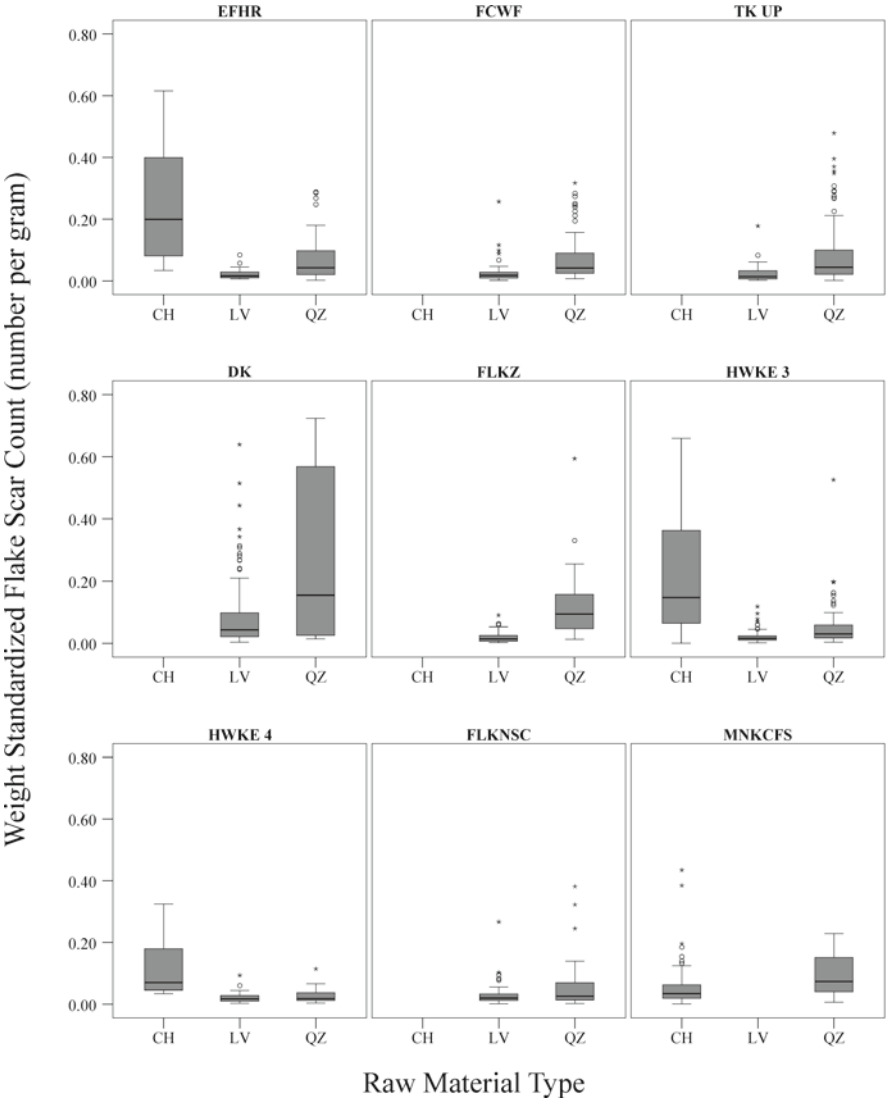

Fig. 8.2 The Bernoulli core model shows mixed results in predicting patterns of Oldowan core reduction intensity. Illustrated are the median, quartiles, and outliers for weight-standardized flake scar counts for Oldowan cores made on three broad types of stone raw material. Raw material quality (i.e., *p*) is generally lowest for quartz/quartzite, somewhat higher for lava materials and is highest for chert. The median and range of core reduction intensity for quartz/quartzite cores is greater than that for lava-based cores, corresponding to the predictions of the Bernoulli core model. However, the median and range of chert core reduction intensity is higher in all but one case, contrary to model prediction. The sample includes nine Olduvai Bed I and Bed II sites. Statistical summaries are based on Kimura (1999, 2002) and additional unpublished data provided by Yuki Kimura

it is now clear why mean reduction intensities increase as the probability of success decreases: Cores based on materials that have a high endogenous probability of success very quickly reach the target utility and are immediately discarded, whereas reduction continues blindly for core-based materials with a low probability of success. These assumptions are clearly flawed. Indeed, the opposite relationships are commonly assumed, namely, that high-quality raw materials will be intensively reduced to extract as many "successes" as possible, whereas low-quality materials will be abandoned at the first possible opportunity.

Markov Core Technology

When should one stop investing in the reduction of a specific stone core? This economic decision is integral to the process of stone core reduction. Unfortunately, such decisions – commonly termed as optimal stopping problems – turn out to be much more complex than they first appear (e.g., Dixit and Pindyck 1994). The complexities underlying the decision of when to stop core reduction stem from the fact that stone raw material fracture is inherently unpredictable: A core that has *so far* proven to be unproductive might eventually reverse this trend and end up by yielding a high return on the investment. In contrast, a core that has *so far* proven to be productive might suddenly become unworkable following a quick succession of reduction errors.

To model the decisions involved in core reduction under these conditions of uncertainty, it is necessary to make different assumptions about the nature of flake production. In contrast to the Bernoulli core model, where I assumed that utility of a removed product was independent of the results of all preceding removals, here I assume that the utilities of detached pieces are sequentially correlated.

$$x_{n+1} = x_n + \delta_n, \tag{8.2}$$

where x_n is the utility of the flake produced at reduction step n in a sequence of N possible removals, x_{n+1} is the utility of next flake in the sequence, and δ_n is a random error (variable) that occurs in the production of the flake at step $n+1$. Note that δ_n may be drawn from any number of different probability density functions. Equation 8.2 describes a simple Markov process where the probability of obtaining a particular utility x_{n+1} is dependent only upon: (1) the results of the event immediately preceding it x_n and (2) the nature of the stochastic process described by the random variable δ.

All future states of the system can be predicted if one understands the stochastic process δ and provided that even a single point x_n is known. Consider the situation where there is no error associated with flake production (i.e., δ=0). The utility achieved with the first removal x_1 is perfectly translated into the utility of the second removal x_2 and, in fact, all subsequent removals, until the core is finally discarded. Ideally, just this sort of "error free" process describes the economic principle behind stone blade technologies; each blade removed sets up the linear ridges that determine the size and shape

of all subsequent removals (Boëda 1995). Yet, situations where $\delta \sim 0$ are probably very rare. Even the most rigorously controlled knapping experiments demonstrate the there is always uncertainty inherent in flake production (Pelcin 1997).

The statistical distribution of errors produced during Markov core reduction may be modeled in a number of different ways. Here, I adopt a model where δ_n can assume one of two values.

$$\delta_n = \begin{cases} +\varepsilon, & p \\ -\varepsilon, & (1-p) \end{cases}. \tag{8.3}$$

Equation 8.3 states that positive errors of size $+\varepsilon$ occur with probability p, whereas negative errors of size $-\varepsilon$ occur with probability $1-p$. Positive errors may be interpreted as unexpected events in flake production that *increase* the utility of the detached product and potentially enhance the utility of subsequent products; sometimes overshooting the core margin not only yields a blade with a longer than expected cutting edge, but also establishes strong core convexities that allow one to remove even longer blades with the next blow. Negative errors, in contrast, are understood to be unexpected events in flake production (e.g., hinge or step fractures) yielding a product of low utility and which may negatively impact the expected utility of future products removed from the core. As with the Bernoulli core model, the probability of a success p may be interpreted as a measure of raw material quality.

Figure 8.3 illustrates how the probability of successful flake production p impacts the process of core reduction. Each panel shows core reduction trajectories simulated by iterating Eq. 8.2 for 100 steps (i.e., flake removals). In all cases, core reduction begins at an utility of zero arbitrary units (AU) (i.e., $x_0 = 0$) and the size of errors is set at $\varepsilon = 0.5$ AU. The only parameter allowed to vary is the probability of success p. Not surprisingly, when p is high the utility of products tends to increase over the course of core reduction (Fig. 8.3a), whereas the utility of products tends to decrease when p is low (Fig. 8.3b). Despite these general trends, there remains substantial variability in the trajectories followed by individual Markov cores. The mean utility of a collection of products derived from Markov cores after n removals is given by $\mu[x_n] = (p-q)\varepsilon n$, where $q = (1-p)$. The variance is given by $\sigma^2[x_n] = 4p(1-p)\varepsilon^2 n$ (Dixit and Pindyck 1994). For example, the expected mean utility of a collection of core products after 100 removals and with $p = 0.8$ is $\mu[x_{100}] = 30$ AU (Fig. 8.3a). The standard deviation in utility for this same collection of products after 100 removals is $\sigma = 4$ AU ($\sigma^2[x_{100}] = 16$ AU^2). The greatest uncertainty in core reduction occurs when $p = 0.5$, which may be interpreted to mean raw materials of intermediate quality. In this case, the products from different core reduction trajectories are expected to have a mean utility after 100 removals of $\mu[x_{100}] = 0$, the same as the initial starting utility, but the standard deviation is $\sigma = 5$ AU ($\sigma^2[x_{100}] = 25$ AU^2) (Fig. 8.3c).

Figure 8.3 also illustrates a key property of Markov processes: If the utility of the current detached piece is high, then the utility of the next piece will also tend to be high, and *vice versa*. This property has predictive value and therefore may be used in coming to a decision about whether to discard a core midway through reduction. In general terms, Markov core reduction should be terminated when the

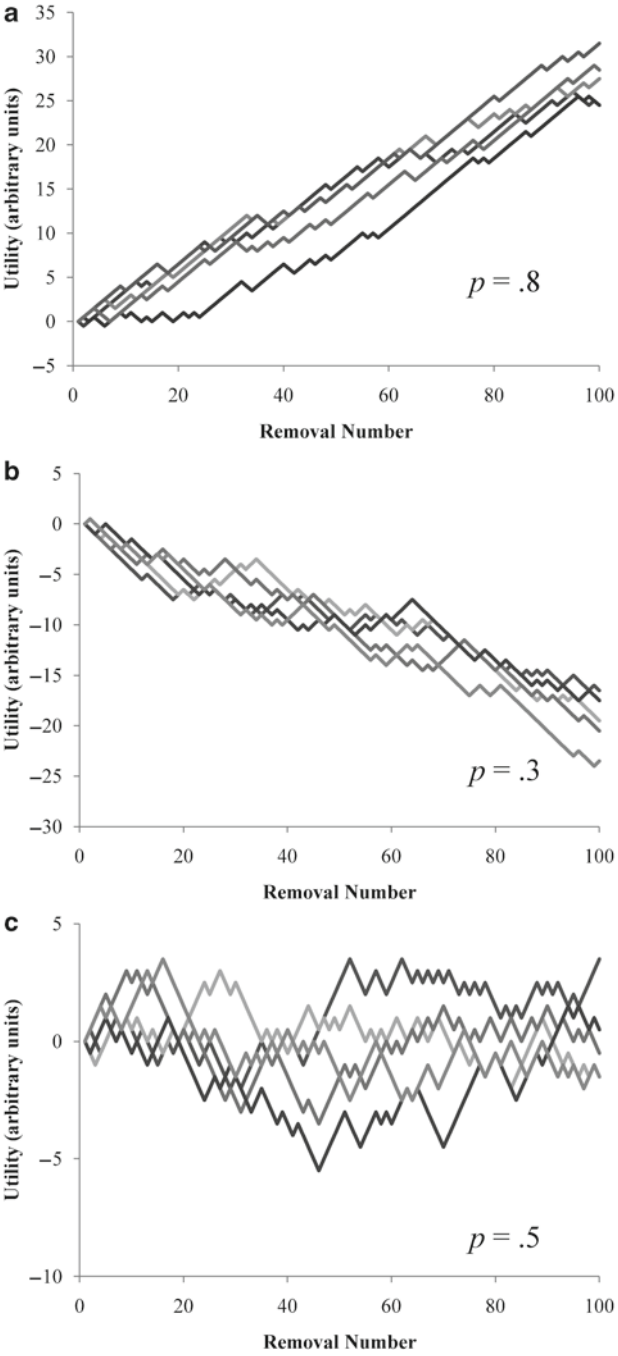

Fig. 8.3 Simulated core reduction trajectories for three raw materials with different error probabilities. The trajectories were generated by iterating Eq. 8.2 with an initial value of $x_0=0$ and $\varepsilon=0.5$. (**a**) When raw material quality is high ($p=0.8$), the utility of detached pieces increases away from the initial value. (**b**) When quality is low ($p=0.3$), utility decreases. (**c**) At intermediate raw material quality ($p=0.5$), some trajectories end up above the starting value ($x_{100}>0$), while others end up below the starting value ($x_{100}<0$)

utility of the current detached piece is perceived to be *too low* because there is a high expectation that the next and, perhaps, all subsequent flakes are also likely to have a utility that is *too low*. More technically, I define a boundary utility x_n^* such that, for each flake removal n in the reduction process, if the utility of the current product $x_n \geq x_n^*$ then core reduction is continued. However, if $x_n < x_n^*$ then reduction is terminated and the core is immediately discarded. Values of x_n^* plotted against removal number n form a boundary curve for the entire reduction process. The boundary curve describes the conditions under which it is optimal to discard the core rather than to continue with a current reduction trajectory.[1]

There are a number analytically demanding approaches to estimating the features of optimal stopping boundary curves (see also Brantingham 2007; Dixit and Pindyck 1994). I develop a simple technique for approximating the shape and location of the boundary curve based on simulation. By iterating Eq. 8.2, I simulate repeated core reduction trajectories consisting of a maximum of 100 reduction steps; i.e., each simulated core has a maximum use life of 100 removals. Simulated core reduction events are partitioned into those that successfully reach a target utility T, defined a priori, and those that did not. T may be equated with common currencies such as cutting edge length or resharpening potential. Returning to Fig. 8.3 as an example, if one arbitrarily sets a target utility $T=5$, then all the trajectories in Fig. 8.3a would be classified as successful in having reached the target, whereas all the trajectories in Fig. 8.3b would be considered unsuccessful. All the reduction trajectories represented in Fig. 8.3c are also ultimately unsuccessful, though one comes very close to reaching T in the last few reduction steps. Define $\min[x_n]$ as the minimum utility observed at each step in the reduction process considered over all of the trajectories that managed to reach the target utility T. Each value of $\min[x_n]$ therefore represents the cumulative value of negative errors, through the removal of n, allowable if a reduction trajectory is to reach the target utility within the use life of the core. In other words, $\min[x_n]$ is how far the mighty core can fall and still have hope of getting back up. I take $\min[x_n]$ to be an approximation of x_n^*. In all instances below, free boundaries were constructed prior to collecting data on discard by simulating 10,000 core reduction events. The free boundary is then interpolated using a nonlinear least squares regression of simulated $\min[x_n]$ against removal number.

Figure 8.4a provides an example of a boundary curve defined using the procedures detailed above. The starting utility is $x_0=0$, probability of a positive error $p=0.5$, error magnitude $\varepsilon=\pm 0.5$, and a maximum number of reduction steps $N=100$. Figure 8.4b illustrates how the boundary curve "weeds out" reduction trajectories headed away from a desired target utility. Note that the evaluation of x_n against x_n^* occurs after each removal in the reduction process and a decision is then made whether to stop or to continue reduction. This procedure is important for two

[1]A boundary curve x_n^* is frequently termed as a "free boundary" because the shape and position of the curve cannot be predicted a priori, but rather result from the unfolding of the random process itself. In the case of core reduction, the approximate features of the free boundary might be known *a priori* as a result of previous experience reducing the raw material in question. However, each piece of raw material will still be unique in many features requiring a dynamic adjustment of the boundary to suit the results of an actual sequence of flake removals.

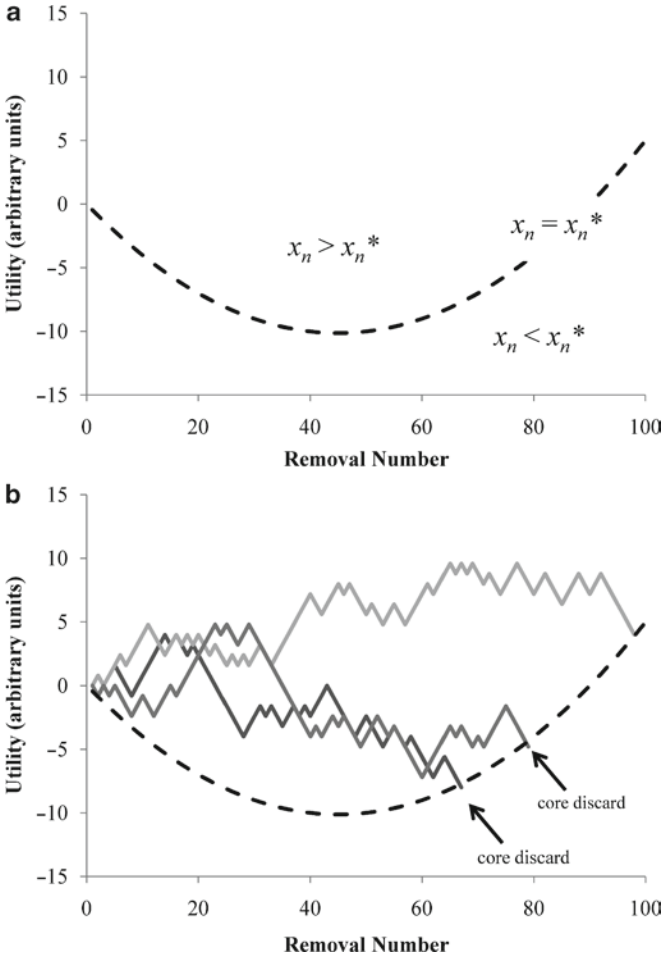

Fig. 8.4 (**a**) A boundary curve divides core reduction into two regions based on whether a trajectory is likely to reach a predetermined utility (e.g., a desired blade length or weight). It is optimal to continue core reduction as long as the utility of a product just removed from a core is greater than the boundary value for that reduction step. (**b**) If the value of a product just removed falls below the boundary value, then the core should be discarded. Simulation parameters: maximum reduction steps $N = 100$; target utility $T = 5$ AU; error size $\varepsilon = 0.5$ AU; and error probability $p = 0.5$

reasons. First, it means that the decision-making process is dynamic in the sense that it is constantly being adjusted to accommodate the results of each flake removal. Second, it provides an effective mechanism for controlling opportunity costs. For example, the first core discard in Fig. 8.4b occurs after observing the utility of removal number 23. Discard at this reduction stage frees up time and energy (equivalent to $N - n = 77$ removals) that may be dedicated to reducing a different core.

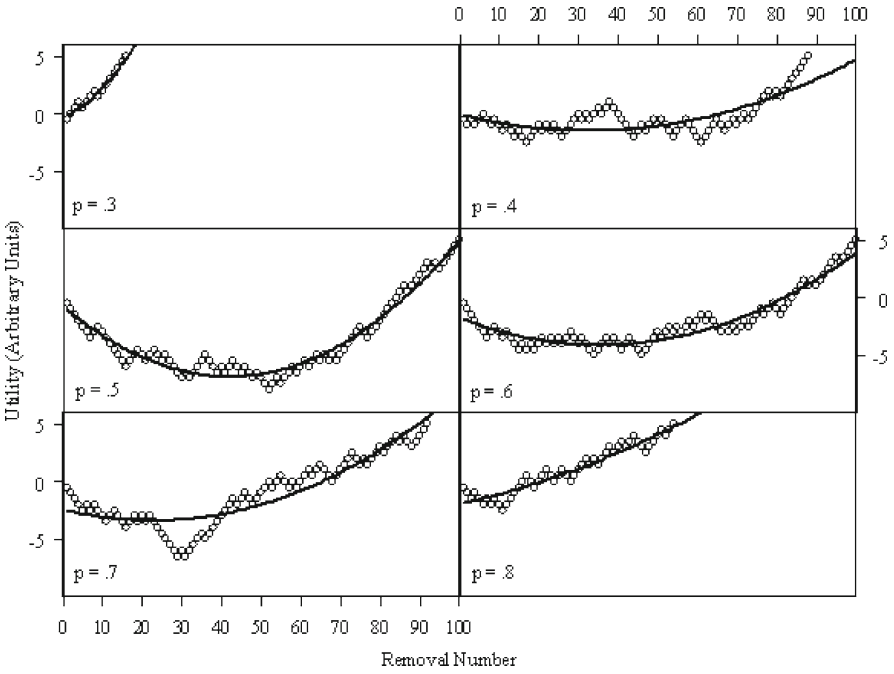

Fig. 8.5 Discard boundary curves (x_n*) for six different values of p. The boundary curves define the optimal points at which to discard a core as a function of the utility of products removed at each stage of reduction (see Fig. 8.4). Boundary curves increase in concavity approaching values of $p=0.5$, but decrease in concavity and increase in slope for values of $p \ll 0.5$ and $p \gg 0.5$. Each boundary curve represents the minimum utilities min[x_n] at each reduction stage n observed among sets of reduction trajectories that hit an arbitrary utility target. Simulation parameters: $x_0=0$ AU; $\varepsilon=0.5$ AU; $N=100$; and $T=5$

The shape of the boundary curve x_n* is dependent upon both the magnitude of reduction errors ε and the probability of encountering a positive error p. Variation in ε alters the concavity of the boundary curve without substantially changing location. Variation in p has a more complex effect and is therefore treated in detail here. Figure 8.5 shows boundary curves computed for core reduction trajectories where the probability of a positive error ranges from $p=0.3$–0.8. When $p=0.3$ (negative errors are approximately 2.3 times more common than positive errors), the boundary curve is very steep and displays positive slopes (Fig. 8.5a). As p approaches 0.5 (negative and positive errors occur with approximately the same frequency), the boundary curve becomes increasingly concave (Fig. 8.5b, c). As p rises above 0.5 (the point where positive errors become more common than negative errors), the boundary curve decreases in concavity and slopes again become more positive (Fig. 8.5d–f).

Despite the superficial similarity between the boundary curves for $p \ll 0.5$ and $p \gg 0.5$, the two boundaries have dramatically different effects on patterns of core

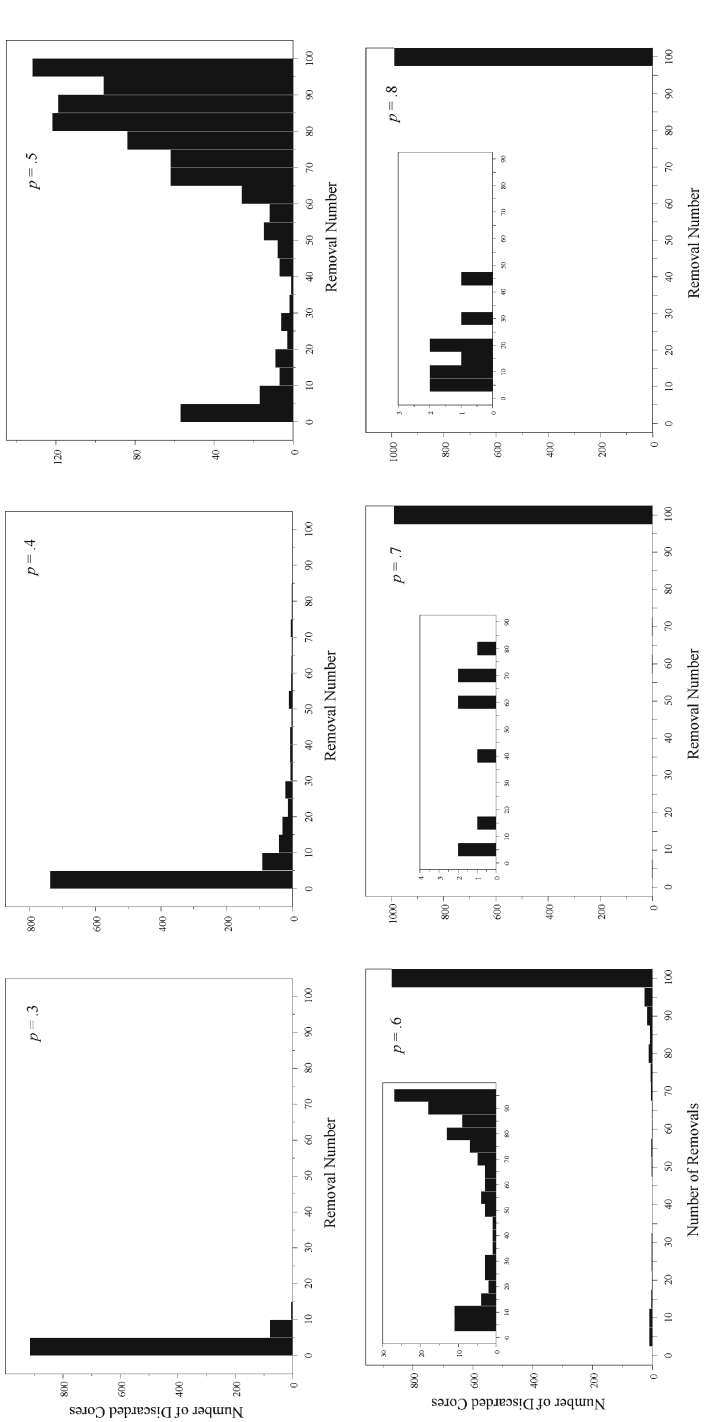

Fig. 8.6 Discard distributions simulated for Markov cores with six different error probabilities. Low-quality materials ($p<<0.5$) generate core discard distributions with a peak at low-reduction intensities and a right-skew dependent upon the value of p. Intermediate quality materials ($p \sim 0.5$) generate a U-shaped discard distribution with many cores discarded both in early and late stages of reduction, but lower numbers discarded at intermediate reduction intensities. High-quality materials ($p>>0.5$) show the majority of cores discarded at high-reduction intensities, but a small number of cores are always discarded at early reduction stages if they accumulate negative errors at a fast initial rate. Data represent 1,000 simulated core reduction trajectories for each value of p. Other parameters are held constant: initial utility $x_0=0$ AU; error size $\varepsilon=0.5$ AU; maximum reduction intensity $N=100$. Cores are discarded at reduction step n if they cross the boundary utility x_n^* or, if they remain above the boundary, at the maximum reduction intensity N. See Fig. 8.4 and text for details. Inset panels show a close-up view of the frequencies of discarded cores at moderate and low-reduction intensities

discard. Using the boundary curves presented in Fig. 8.5, I simulated core reduction and discard following the procedure shown in Fig. 8.4b; core reduction trajectories are generated by iterating Eq. 8.2 and core discard is recorded either when (1) the reduction trajectory contacts the discard boundary or (2) if the maximum number of removals N have been obtained. Figure 8.6 presents frequency distributions of the discard stages (i.e., number of removals n at discard). Each panel tabulates the results for 1,000 simulated reduction trajectories for six different values of p, with $x_0 = 0$ AU, $\varepsilon = 0.5$ AU, and a maximum core use life $N = 100$. The shape of the discard distributions is substantially different from that generated by the Bernoulli core model (compare to Fig. 8.1a).

First, note that none of the discard distributions are normal (Gaussian) in shape. Rather, core discard patterns are right skewed for values of $p \ll 0.5$, with the strength of the skew increasing as p increases. In other words, as p (i.e., raw material quality) increases toward 0.5, there is an increasing tendency for cores to be reduced farther, though the majority of cores are still discarded almost immediately after reduction begins. The reason for the peak in discard at very low-reduction intensities is that boundary curves for low p effectively track the rate at which positive errors accumulate. If positive errors do not accumulate fast enough (a rate greater than or at least proportional to the slope of x_n^*) then a core is discarded. At low p, this condition is very strict (i.e., slope of x_n^* is large and positive).

As p approaches 0.5, the discard distribution takes on a strong U-shape, with large numbers of cores being discarded both at low- and high-reduction intensities and an even representation of cores at intermediate reduction intensities. The peak in core discards at low-reduction intensities represents the boundary curve "weeding out" those cores that accumulate negative errors too quickly as reduction begins – the negative error accumulation rate exceeds the slope of x_n^*. In contrast, the peak in core discards at high-reduction intensities represents "weeding out" based on an insufficient positive error accumulation rate. The intermediate region defined by relatively low, but even core discard reflects a tolerance for the accumulation of some negative errors over the course of core reduction. Most of the correction of these errors is accomplished either early or late in reduction, but not in between.

Contrary to what might be expected given the simulated discard patterns for $p \ll 0.5$, the distribution of core discard for $p \gg 0.5$ is not left skewed. As p increases above 0.5, core discards increasingly concentrate in two zones, a very large peak at high-reduction intensities and a small peak at low-reduction intensities. The distribution looses all traces of core discards at intermediate reduction intensities.

Evaluating the Markov Core Model

The Markov core model is perhaps best suited to describing core technologies that exploit the relationship between the morphology of flake scars to predetermine the size and shape of subsequent removals. Levallois technologies are the earliest and best-known

core technologies to make use of such relationships. In particular, Van Peer (1992) has shown using extensive refits that the microtopography of flake scar ridges correspond to the shapes of Levallois products removed from cores. In the case of centripetal Levallois technology, ridges from more than one previous flake removal play a role in determining the size and shape of a single Levallois product. The Markov model as presented above may be a bit of a stretch in this case. However, the assumptions of the Markov core model seem more appropriate for Levallois blade technologies, where each blade removed establishes a linear ridge which serves as a template for the next blade.

Shuidonggou, an early Upper Paleolithic site in Northwest China dating to ca. 25 ka, is dominated by Levallois blade technology based predominantly on alluvial cobbles of silicified limestone (Brantingham et al. 2001). Since the Markov core models make predictions about the distribution of reduction intensity across cores, it is necessary to derive such a measure for the Levallois blade cores recovered from Shuidonggou. Here, I use core remnant use life, which is an estimate of the number of blades that could have been removed from a core if it had not been discarded. Remnant use life is calculated as the core thickness minus the expected thickness of the "slug" of unusable material remaining when a core is completely spent. The typical "slug" at Shuidonggou is 20 mm thick (Brantingham 1999). The usable material in a discarded core is then divided by the average Levallois blade thickness observed in the assemblage. At Shuidonggou, the average thickness of Levallois blades is 7.6 mm. Remnant use life is a measure of the number of additional blades that could have been removed from a core had it not been discarded. The results are presented in Fig. 8.7 for unidirectional and bidirectional Levallois blade cores.

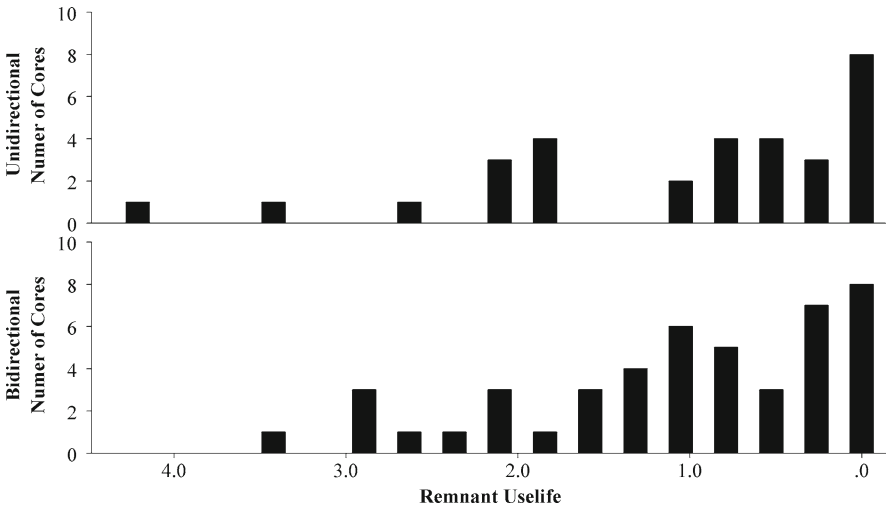

Fig. 8.7 Remnant use life measured for unidirectional and bidirectional blade cores from the Shuidonggou early Upper Paleolithic site, China. Remnant use life is an estimate of the number of blades that could potentially be removed from a discarded core. It is calculated as the discarded core thickness minus the average thickness of the "slug" of unusable raw material in a spent core (~20 mm). The resulting value is then divided by the average thickness of blades seen at the site (~7.6 mm)

Reduction intensity of Levallois cores at Shuidonggou meets some of the expectations of the Markov core model. In particular, the distribution of remnant use life is positively skewed with an increasing number of cores reduced close to the maximum (Fig. 8.7). In comparison with the simulations presented in Fig. 8.6, reduction of silicified limestone appears to be similar in some ways to an error process with $p \gg 0.5$; i.e., silicified limestone is a high-quality raw material which produces many more positive than negative errors during reduction.[2] Remnant use life does not appear to be similar to the "U-shaped" profiles of intermediate quality materials (i.e., $p \sim 0.5$) (but see below), nor the negative skew reduction intensity distributions of low-quality raw materials ($p \ll 0.5$). However, observed remnant use life among discarded Levallois cores at Shuidonggou is unlike the simulated distributions with $p \gg 0.5$ in that it increases gradually. Simulated reduction intensity for $p \ll 0.5$ show many more cores – sometimes an order of magnitude more at the simulated sample sizes – making it all the way through the reduction process.

The observed distribution of remnant use life at Shuidonggou could be most similar to the "U-shaped" profile for intermediate quality materials, but without the branch of the "U" representing cores discarded early in the reduction process. This possibility should not be surprising since Fig. 8.7 considers only cores that can be typologically classified as Levallois blade cores. Many cores that were discarded early in reduction may be nondiagnostic since they have not accumulated enough attributes to be unequivocally assigned to a Levallois reduction strategy. Nevertheless, such nondiagnostic cores may have been started with the intention of producing a Levallois blade core. This may be a safe assumption for nondiagnostic cores in the Shuidonggou assemblage. More than 57% (68 of 119) cores based on silicified limestone are formally classified as Levallois blade cores and 16% (19 of 119) are classified as polyhedral. However, including nondiagnostic silicified limestone cores among the diagnostic Levallois blade cores does not change the overall shape of the remnant use life distribution (Fig. 8.8). Thus, while the Markov core model may offer a reasonably close approximation of the decision-making process involved in Levallois blade core reduction at Shuidonggou, the observed differences with theoretical expectations suggest that a more sophisticated model is probably required.

Price Core Technology

Most lithic specialists would agree that the decision making that takes place during core reduction involves much more than simply deciding when to abandon a core that is proving to be unproductive. Rather, most core reduction strategies combine multiple, distinctive flaking actions that are combined in different proportions to achieve different economic goals. Indeed, it is possible to view the design of core technologies as the assembly of different flaking actions over the use life of the core.

[2] Note that direction of the axes in Figs. 8.7 and 8.8 are reversed so that reduction intensity increases towards the right.

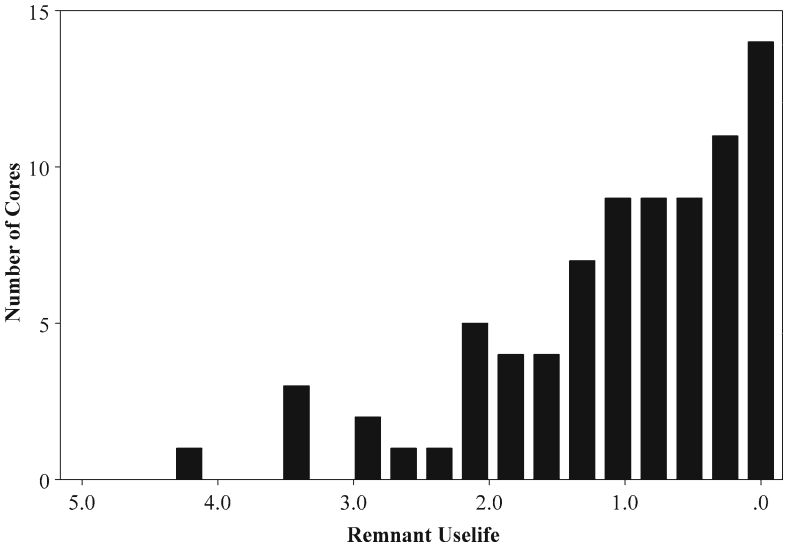

Fig. 8.8 Remnant use life of formal Levallois blade cores and nondiagnostic cores based on silicified limestone from Shuidonggou

It is possible to model this more complicated situation by attributing to the knapper the ability to weigh the results from different, unique flaking actions, and adjust the proportions at which those flaking actions are deployed at the next reduction step. Consider a collection of different possible flaking actions that we label $i = 1, 2, \ldots I$. Each flaking action might be distinctive because of the type of percussor used, magnitude of force applied, angle of impact, location on the core, and so on. Each flaking action i produces k_{in} flakes at reduction step n and a total number of $K_n = \sum k_{in}$ flakes are produced by all the flaking actions at the reduction step. Let $p_{in} = k_{in}/K_n$ be the proportion of flakes produced by the flaking action i at reduction step n and define x_{in} as the utility of the flakes produced by action i at step n. The mean utility of all flakes produced at reduction step n is then $x_n = \sum p_{in} x_{in}$.

Given these model elements, changes in a core reduction strategy might originate in two ways. First the utility of flakes produced by each strategy might change as a result of an error process like that defined for Markov core technologies.

$$x_{in+1} = x_{in} + \delta_{in}. \tag{8.4}$$

Here, the utility of flakes produce by action i at reduction step $n+1$ is determined by the utility of flakes at step n and some random error δ_{in} drawn from a probability distribution. Unlike the Markov core model presented above, I will assume here that δ_{in} is drawn from a normal distribution with some mean μ and standard deviation σ (see Brantingham 2007). If $\mu > 0$, then errors will tend to be positive more often than negative and will lead the utility of flakes x_{in} to increase. If $\mu < 0$, then errors will tend to be negative and x_{in} will decrease. The sign of μ may be interpreted

as a measure of raw material quality and σ as a measure of the inherent variability in quality of a raw material package.

Second, change may be accomplished by altering the proportions of different flaking actions used at each reduction step. Let w_{in}/w_n be the relative payoff a knapper associates with the flakes produced by action *i*. Note that relative payoff is the absolute payoff w_{in} divided by the mean payoff over all flaking strategies $w_n = \sum p_{in} w_{in}$. For the sake of simplicity, w_{in}/w_n is taken to be a positive linear function of utilities x_{in}

$$\frac{w_{in}}{w_n} = \frac{\alpha}{w_n} x_{in} + \frac{\beta}{w_n} \tag{8.5}$$

meaning that as the utility of flakes associated with action *i* increases so does the relative payoff assigned to action *i* by the knapper. Thus, the proportion of flakes produced by flaking action *i* in the next reduction step changes as

$$p_{in+1} = p_{in} \frac{w_{in}}{w_n}. \tag{8.6}$$

Since the function describing the relative payoffs associated with different flake utilities is positive, those flaking actions that yield higher relative payoffs (i.e., $w_{in}/w_n > 1$) will come to occupy a dominant proportion of the core reduction strategy. Those flaking actions yielding flakes with lower relative payoffs (i.e., $w_{in}/w_n < 1$) will become proportionally rare in the reduction strategy.

It is possible to combine Eqs. 8.5 and 8.6 to yield a classic replicator equation describing both stochastic sources of change from raw material quality and deterministic sources of change from decisions implemented by the knapper

$$p_{in+1} x_{in+1} = p_{in} \frac{w_{in}}{w_n} \left(x_{in} + \delta_{in} \right). \tag{8.7}$$

Equation 8.7 describes the proportion of the core reduction strategy and the utility associated with flakes produced by flaking action *i* in the next reduction step $n+1$ given both selection among flaking actions by the knapper *and* stochastic effects of the raw material. Note that there is one such equation for each unique flaking action deployed within a core reduction strategy and that each equation is tied together by the relative payoffs attributed to each flaking action. Figure 8.9 shows the change in the fractional utility for flakes produced by ten different flaking actions over the course of reduction of a single core. Each of the ten flaking strategies initially comprises $p_{in} = 0.1$ of the total core reduction strategy and the fractional utility of each strategy is $p_{in} x_{in} = 10$. The mean utility of the core at the start of reduction is $x_n = \sum p_{in} x_{in} = 100$ (see below). After about 15 removals, the simulated knapper begins to select for those flaking actions that produce higher payoffs and select against those that do not. Seven of the ten initial flaking strategies are no longer deployed by around reduction step 30 and the core reduction strategy consists of three dominant flaking actions. These fluctuate in prominence over the remainder of reduction; action 5 dominates between steps 32 and 69, action 2 between steps 70 and 87, and action 1 between

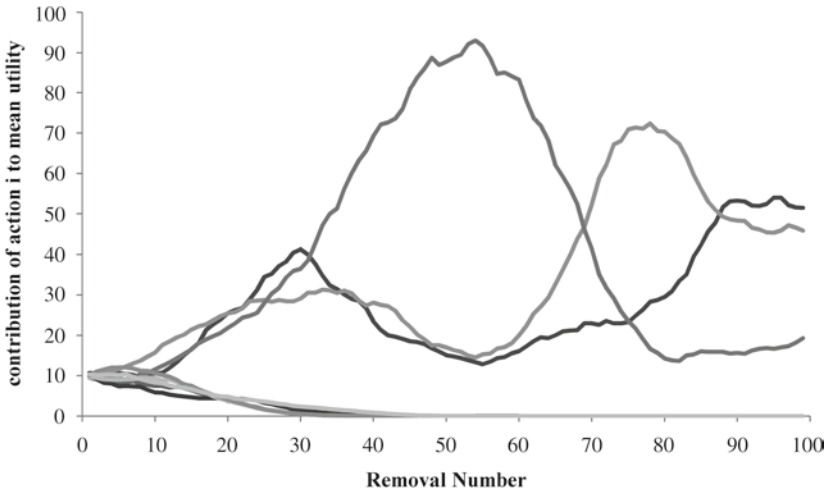

Fig. 8.9 Simulated fractional utilities of flakes produced by ten unique flaking actions in the reduction of one core. Fractional utilities are the proportion of the total strategy made up by action i multiplied by the utility of the flakes from action i at each reduction step (i.e., $p_{in}x_{in}$). The payoff function used in simulated core reduction is $w_{in}=0.5x_{in}+1$ (both sides divided by mean payoffs w) and the error process for δ is a normal distribution with mean $\mu=0$ and standard deviation $\sigma=1$

step 88 and the discard of the spent core at step 100. The dynamic shifting of different flaking action over the course of the reduction of a single core is at least qualitatively like what is seen for real core technologies (Baumler 1995; Volkman 1983).

However, it is clear that it would be cumbersome to track the trajectory of each flaking actions, even if they were deployed in modest numbers. Moreover, it is debatable whether the decision to discard a core is based on the results of flakes produced by individual flaking actions, independent of the others. Some aggregate measure of core productivity is perhaps more appropriate. Fortunately, we can draw on a very important result from the mathematics of selective processes to describe the evolution of the reduction process in terms of the rate of change in the mean utility of the core (see Brantingham 2007; Frank 1997; Price 1970; Rice 2004).

$$\Delta x = \mathrm{COV}\left[\frac{w_{in}}{w_n}, x_{in}\right] + E\left[\delta_{in}\right]. \tag{8.8}$$

Equation 8.8 is the Price equation (Price 1970) and, in homage, I call the modeled core technology a Price core. Equation 8.8 is derived directly from Eq. 8.7. It partitions the rate of change in the mean utility of a core into: (1) a covariance component describing how the knapper weighs relative payoffs associated with flakes produced by each flaking action and (2) the expected effects of errors (i.e., raw material quality).

There is a vast number of ways in which we could model a Price core technology by parameterizing different payoff functions (Eq. 8.5) and probability distributions describing the character of errors produced during core reduction. This is clearly

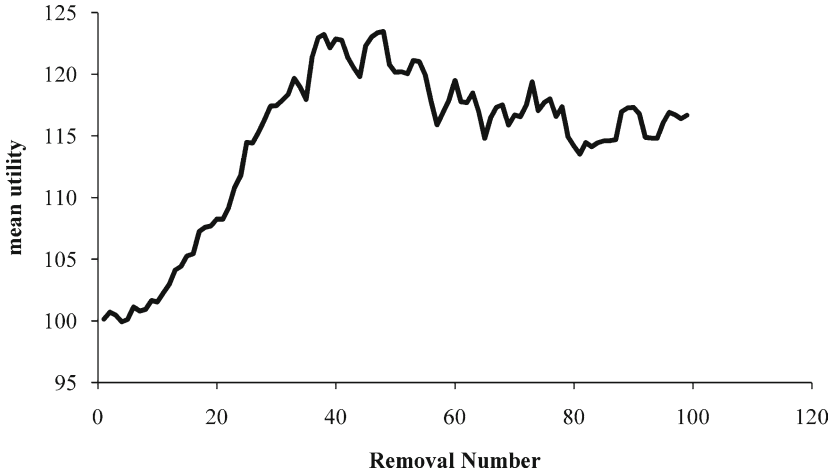

Fig. 8.10 Simulated mean utility of flakes produced in the reduction of one Price core

beyond the scope of this chapter. A quick look at the dynamics of Eq. 8.8, however, suggests that if the sum of the covariance term and the expectation term is positive, then the mean utility of the core will increase regardless of specific parameterizations of the model. An increasing mean utility can happen if both terms of Eq. 8.8 are positive, meaning that both the knapper's ability to select among different flaking actions and raw material quality tend to enhance the utility of flaking products. Mean utility will also increase if one term is positive and the other is negative, but the positive term is much larger. In other words, a very skilled knapper can adjust flaking actions to overcome poor raw materials (i.e., $\mathrm{COV} \gg 0$ and $E < 0$), or a good raw material can make even a mediocre knapper look great (i.e., $\mathrm{COV} < 0$ and $E \gg 0$). Figure 8.10 shows how the selection among the different flaking actions in the case of the simulated core in Fig. 8.9 leads to an increase in mean utility of the flaking products. Here $E[\delta] = \mu = 0$ and all the directionality in the mean utility is the result of a positive covariance between payoffs w_{in}/w_n and utilities x_{in}.

Evaluating the Price Core Model

The last point above suggests that a knapper may be able to select among different flaking actions to steer a core clear of the free boundary which, in the case of the Markov cores described earlier, might be used to decide when to discard a core. Figure 8.11 shows this to be the case for 500 simulated cores where the criterion for core discard is similar to that for Markov cores, namely when the mean utility removed products from a core x_n at reduction step n falls below a mean free boundary x_n^*. The simulated Price cores in Fig. 8.11 have payoff function shown with slope $\alpha/w_n = 2$ (Eq. 8.5), mean error distribution is $\mu = 0$ and standard deviation is $\sigma = 2$. Interestingly, the raw material quality as modeled here is based on a normal

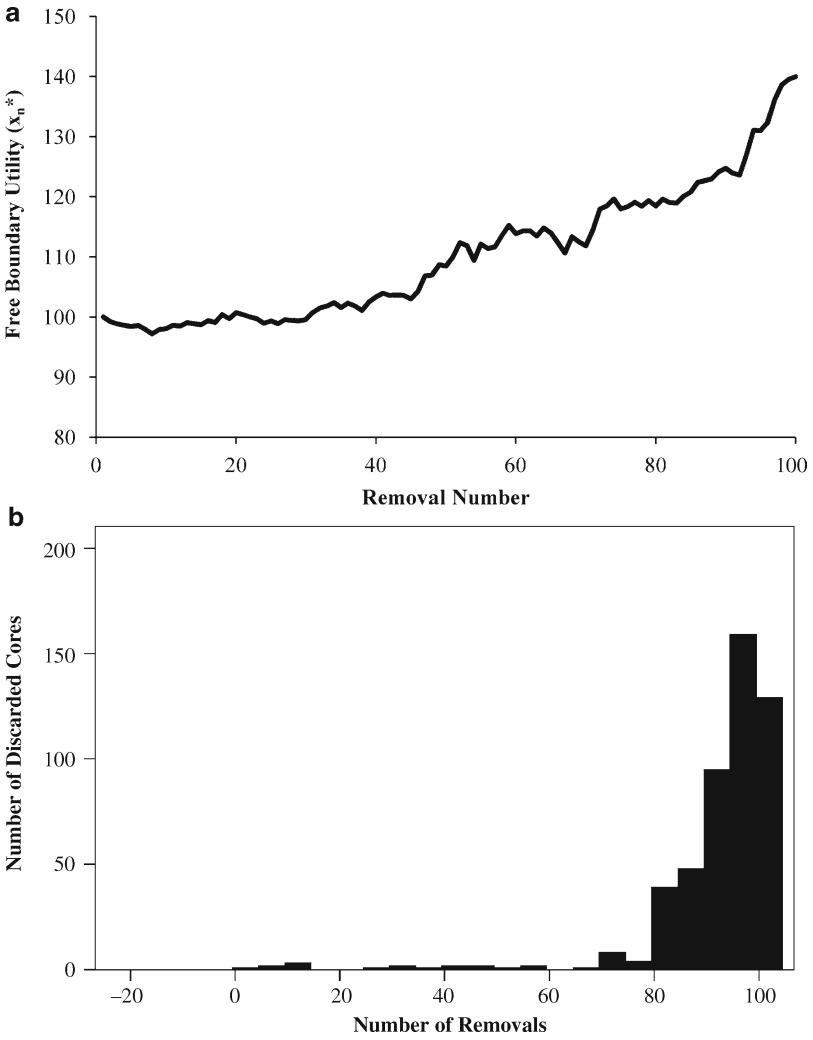

Fig. 8.11 The simulated free boundary (*top*) for Price cores where there is a slight positive payoff function allowing knappers to selecting between different flaking strategies and an error distribution with a mean of zero and a standard deviation of two (moderate quality raw material). The discard distribution for simulated cores (*bottom*) shows a gradual increase in the number of discarded cores as one approaches the end of the use life of each core. The simulated distribution is qualitatively similar to that seen for Levallois blade cores at Shuidonggou

distribution with a mean of zero is conceptually similar to the Markov core example with the probability of a positive error $p = 0.5$; i.e., positive and negative errors occur with approximately equal frequency. However, the free boundary in the case of the Price core modeled here is much more similar to that for a raw material of much higher quality (see Fig. 8.5 where $p = 0.7$). This provides casual confirmation that the ability to select between different flaking actions can outweigh the effects

of raw material quality. However, the impact on core discard distributions is not directly comparable. Here, we see a single-tailed distribution with the number of discarded cores increasing gradually as the maximum core use life is approached. In contrast, for the Markov cores modeled above, any value of $p > 0.5$ shows most cores being discarded at maximum use life. The resemblance between the simulated discard distribution for Price cores and the remnant use life distributions for Levallois blade cores from Shuidonggou is striking (see Figs. 8.7 and 8.8). While this does not necessarily confirm that Levallois blade technology at Shuidonggou follows a Price core reduction strategy, it does suggest that further modeling work is warranted.

Conclusions

The goal of this chapter is to develop a series of formal mathematical and simulation models to account for the variability in the intensity of reduction observed across different stone core technologies. Three models were presented each of which made increasingly complex assumptions about the decision-making process deployed during the course of reducing a mass of raw material. The models may be thought of in an evolutionary light, though no implications about long-term patterns of stone technological change were derived. The three models were compared with data on core reduction intensity from Olduvai Gorge and Shuidonggou, an early Upper Paleolithic site in Northwest China dating to approximately 25 ka.

Bernoulli core technology was developed as a model of reduction where the utility of flakes produced is binary (i.e., good or bad), the probability of obtaining a good flake is fixed by stone raw material quality, and each flake removal is independent of all other flake removals. Bernoulli core reduction proceeds until the knapper obtains some predetermined number of good flakes, and the prediction is that poor quality raw materials will be reduced much more intensively than high-quality raw materials because it takes much longer to produce the desired number of good flakes. This prediction is contrary to the general assumption made by lithic technologists. Comparison with data on weight-standardized flake scar counts for several sites from Olduvai Gorge suggests that Oldowan core technology is not a Bernoulli core technology. In particular, it is possible to reject the hypothesis that poor quality raw materials are more intensively reduced. Rather, the opposite reduction pattern appears to hold – higher-quality materials are more intensively reduced – suggesting that Olduvai hominins were making decisions to discard cores that were not proving to be economically productive. This level of decision making is consistent with recent evidence of very selective raw material use (Stout et al. 2005) and evidence for surprisingly sophisticated approaches to core reduction (Delagnes and Roche 2005).

Markov core technology is a model that accounts for decisions to discarded cores before they have reached some predetermined target utility. The Markov core model also posits flakes produced in a sequence are not statistically independent of one another, but rather the utility of a flake just removed from a core is partially

determined by the utility of the preceding flake along with some error that arises from the quality of the raw material being reduced. This assumption leads to a dynamic model where the utilities of flakes removed from a core perform a random walk. If we define some threshold utility that the knapper is trying to achieve through core reduction, then it is possible to learn about reduction trajectories that do not reach this threshold and set up a set of criteria that would cue the knapper that a given core was not likely to reach the desired threshold utility. In technical terms, the set of cues used to decide that a core is not likely to reach a threshold utility is called a free boundary. Simulation suggest that core reduction that incorporates an autocorrelation of flake utilities and allows for core discard if the utility of a flake falls below the free boundary lead to very distinctive core discard patterns. In particular, for intermediate quality raw materials where positive and negative errors are equally likely to occur, the frequency of cores discarded at different reduction intensities should be "U-shaped"—many cores minimally reduced, few cores at intermediate reduction intensities and many cores that are intensively reduced. If negative reduction errors are more common than positive errors, then most cores are discarded very early during reduction. The opposite is true for materials that produce more positive errors than negative. Here, most cores are reduced to a complete spent state. Comparisons of expectations with data on remnant use life among Levallois blade cores from the early Upper Paleolithic site of Shuidonggou, Northwest China, suggest that the Markov core model is closer to the mark. However, the discard pattern at Shuidonggou suggests a gradual increase in the probability that a core is discarded as one approaches the maximum reduction intensity.

The model of Price core technology builds on the Markov model in adding into the system the possibility that core reduction strategies are mixtures of several independent types of flaking actions, and allowing the knapper to selectively deploy these flaking actions depending upon the utility of the flakes each produces. Raw material quality also plays an important role here in generating the variability between different flaking actions. The Price core model generates an interesting picture of core reduction as a sequence of dynamic shifts in the importance of different flaking actions over the course of reduction; some actions predominate early, others take over during intermediate stages and still others are common toward the end of the use life of a core. The Price equation—after which this core technology is named—is derived from the different elements discussed above and provides clues about the interaction between the knapper's ability to steer core reduction in different directions and the impact of raw material quality. Indeed, I propose that the Price equation provides an interesting way of conceiving of stone technological design (see also Brantingham 2007):

$$\Delta x = \underbrace{\mathrm{COV}\left[\frac{w_{in}}{w_n}, x_{in}\right]}_{\text{core technological design}} + \underbrace{E\left[\delta_{in}\right]}_{\text{raw material quality}} .$$

Clearly, much more work has to be done to flesh out this suggestion. However, it is encouraging to note that a Price core simulated discard distribution—using as a

criterion to discard the point where the mean utility of flake products crosses a free boundary – resembles much more closely the observed pattern of core remnant use life seen at Shuidonggou than simpler models.

Acknowledgments This work was inspired by Huberman et al. (1998), showing that inspiration can come from anywhere. I am indebted to Yuki Kimura who provided raw data on flake scar counts and core weights from the Olduvai sites she examined in her dissertation. Todd Surovell and Matt Grove kindly provided helpful comments on a previous version.

References

Bamforth, D.B., 2002. High-tech foragers? Folsom and later Paleoindian technology on the Great Plains. *Journal of World Prehistory* 16: 55–98.

Baumler, M.F., 1995. Principles and properties of lithic core reduction: implications for Levallois technology. In *The Definition and Interpretation of Levallois Technology*, edited by H.L. Dibble and O. Bar-Yosef, pp. 11–23. Prehistory, Madison.

Beck, C., Taylor, A.K., Jones, G.T., Fadem, C.M., Cook, C.R. and Millward, S.A., 2002. Rocks are heavy: transport costs and Paleoarchaic quarry behavior in the Great Basin. *Journal of Anthropological Archaeology* 21: 481–507.

Boëda, E., 1995. Levallois: a volumetric construction, methods, a technique. In *The Definition and Interpretation of Levallois Technology*, edited by H.L. Dibble and O. Bar-Yosef, pp. 41–68. Prehistory, Madison.

Brantingham, P.J., 1999. *Astride the Movius Line: Late Pleistocene Lithic Technological Variability in Northeast Asia*, University of Arizona, Unpublished PhD Dissertation.

Brantingham, P.J., 2007. A unified evolutionary model of archaeological style and function based on the Price Equation. *American Antiquity* 42: 395–416.

Brantingham, P.J., Krivoshapkin, A.I., Li J. and Tserendagva, Y., 2001. The initial Upper Paleolithic in Northeast Asia. *Current Anthropology* 42: 735–746.

Brantingham, P.J. and Kuhn, S.L., 2001. Constraints on Levallois core technology: a mathematical model. *Journal of Archaeological Science* 28: 747–761.

Braun, D. R., Tactikos, J.C., Ferraro, J.V., Arnow, S.L. and Harris, J.W.K., 2008. Oldowan reduction sequences: methodological considerations. *Journal of Archaeological Science* 35: 2153–2163.

Delagnes, A. and Roche, H., 2005. Late Pliocene hominid knapping skills: the case of Lokalalei 2C, West Turkana, Kenya. *Journal of Human Evolution* 48: 435–472.

Dibble, H.L., 1995. Middle Paleolithic scraper reduction: background, clarification, and review of the evidence to date. *Journal of Archaeological Method and Theory* 2: 299–368.

Dibble, H.L. and Bar-Yosef, O., 1995. *The Definition and Interpretation of Levallois Technology*. Prehistory Press, Madison.

Dixit, A.K. and Pindyck R.S., 1994. *Investment Under Uncertainty*. Princeton University Press, Princeton, NJ.

Elston, R.G. and Brantingham, P.J., 2003. Microlithic technology in Northeast Asia: a risk minimizing strategy of the Late Paleolithic and Early Holocene. In *Thinking Small: Global Perspectives on Microlithization*, edited by R. G. Elston and S. L. Kuhn, pp. 103–116. Archaeological Papers of the American Anthropological Association, No 12, Washington, DC.

Frank, S.A., 1997. The Price Equation, Fisher's fundamental theorem, kin selection, and causal analysis. *Evolution* 51: 1712–1729.

Huberman, B.A. et al., 1998. Strong regularities in World Wide Web surfing. *Science* 280:95–97.

Kimura, Y., 1999. Tool-using strategies by early hominids at Bed II, Olduvai Gorge, Tanzania. *Journal of Human Evolution* 37: 807–831.

Kimura, Y., 2002. Examining time trends in the Oldowan technology at Beds I and II, Olduvai Gorge. *Journal of Human Evolution* 43: 291–1321.

Kuhn, S.L., 1994. A formal approach to the design and assembly of mobile toolkits. *American Antiquity* 59: 426–442.

Kuhn, S.L., 2004. Evolutionary perspectives on technology and technological change. *World Archaeology* 36: 561–570.

Lycett, S.J., 2008. Acheulean variation and selection: does handaxe symmetry fit neutral expectations? *Journal of Archaeological Science* 35: 2640–2648.

Nelson, M.C., 1991. The study of technological organization. *Archaeological Method and Theory* 3: 57–100.

Pelcin, A.W., 1997. The effect of core surface morphology on flake attributes: evidence from a controlled experiment. *Journal of Archaeological Science* 24: 749–756.

Potts, R., 1991.Why the Oldowan? Plio-Pleistocene tool making and the transport of resources. *Journal of Anthropological Research* 47: 153–176.

Price, G.R., 1970. Selection and covariance. *Nature* 227: 520–521.

Rice, S.H., 2004. *Evolutionary Theory: Mathematical and Conceptual Foundations*. Sinauer, Sunderland, MA.

Stout, D., Quade, J., Semaw, S., Rogers, M.J. and Levin, N.E., 2005. Raw material selectivity of the earliest stone toolmakers at Gona, Afar, Ethiopia. *Journal of Human Evolution* 48: 365–380.

Toth, N.P., 1982. *The Stone Technologies of Early Hominids at Koobi Fora: An Experimental Approach*. Unpublished PhD, University of California, Berkeley.

Van Peer, P., 1992. *The Levallois Reduction Strategy*. Prehistory Press, Madison.

Volkman, P., 1983. Boker Tachtit: core reconstruction. In *Prehistory and Paleoenvironments in the Central Negev, Israel The Avdat/Aqev Area*, edited by A.E. Marks, pp. 127–190. Southern Methodist University Press, Dallas.